# Calculating Muzzle Motions of the Rifle Barrel

James A. Boatright

Jim@BBLLC.INFO

## 1. Recoil Effects on the Rifle Barrel

In accordance with Newton's Third Law of Motion, initial-stage rifle recoil (before bullet exit) occurs only in reaction to the forward acceleration of the rifle bullet (together with a small portion of the powder charge) during the firing of the rifle. Rifle recoil does not commence until after the rifle bullet has been engraved with the rifling pattern and is free to accelerate down the bore. The line-of-action of this rearward recoil force acting on the rifle is coaxial with the bore of the rifle barrel. In interior ballistics, this recoil force acting rearward on the rifle can be well quantified at any time after bullet engravement as being equal in magnitude and opposite in direction to the base-pressure driving the bullet forward multiplied by the cross-sectional area of the bore being obturated by that bullet. After initial engraving of the rifle bullet by the rifling lands, the forward-acting force of barrel friction is typically less than 2-percent of the bullet's driving force and is thus considered negligible here.

This rearward recoil force on the rifle can be envisioned as being applied primarily to the rifle at the center of its breech face as a significant portion of the thrust of the cartridge case head (and primer) against that breech face plus whatever secondary rearward-acting frictional force might pertain between the outside walls of the cartridge case and the chamber walls.

The CG of most shoulder-fired rifles being fired in an upright position is located several millimeters ($d_{CG}$) vertically below the axis of its bore. Thus, the recoil force briefly creates a barrel-bending torque impulse acting vertically upward at the front face of the receiver upon the rear shoulder of the (assumed) free-floating rifle barrel. Here, we are analytically treating this upward torque impulse as being approximately of a Gaussian shape (a normal probability distribution function) in the time domain, with its peak occurring at the instant of peak base-pressure

driving the bullet forward in the rifle barrel. Peak base-pressure normally occurs when the bullet has moved just a few inches into the bore.

This analytical treatment allows the reasonably precise formulation of the barrel's dynamic response at its muzzle to this torque impulse being applied at its receiver end. We are not concerned here with the muzzle of the barrel being dragged straight rearward during recoil. Good rifle design and firing technique should eliminate any disturbance of the rifle barrel in the horizontal plane during firing, leaving only vertical plane motions to be formulated here.



—— .338 Lapua Mag. - .338, 245.3 gr, ULD(Mk IIb) - 92.0 grs Vihtavuori N565 *C - OAL= 4.175 in.
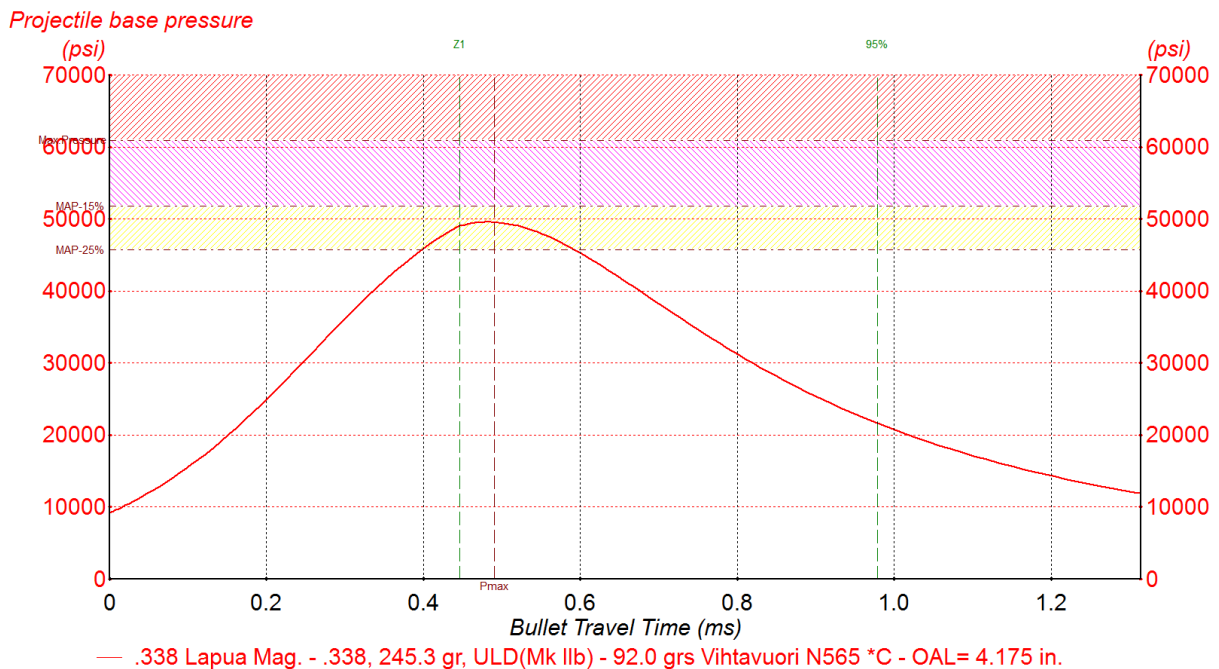
Closely inspecting the base-pressure curve plotted against time in a good interior ballistics application such as QuickLOAD©, we see that it does indeed appear distinctly Gaussian in its excitation profile, having a "standard deviation" spread function, **Sigma(μ-sec)**, given by its rise time in **microseconds (μ-sec)** from **60.65-percent** to **100-percent** of the peak base-pressure $P_{BP}$. We are not concerned here with the slightly skewed shape of this base-pressure curve because we are mainly interested in the rising limb of this base-pressure function. The dashed red vertical line in this QL graph shows the time of peak chamber pressure ($P_{Max}$) which occurs just after peak base-pressure $P_{BP}$. As the bullet moves down the barrel at velocity **V(t)**, its driving base-pressure is

approximated by the instantaneous chamber pressure **P(t)** minus a dynamic pressure, $0.5 \rho V^2$.

This recoil-induced, bending torque impulse acting upon the shoulders of the barrel imparts a time-reversed, approximately Gaussian-shaped transverse shear-wave in a vertical plane into the material of the rifle barrel at its junction with the receiver face. This transverse shear-wave travels toward the muzzle at its own invariant linear propagation rate in the (assumed isotropic steel) material from which the barrel is made. For the rifle barrel as a "long, slender rod," its longitudinal shear-wave propagation rate is given by the square root of the shear modulus of elasticity (**G**) divided by the density (**ρ**) for the barrel steel material. This wave speed is not affected by moderate barrel taper.

The driving recoil torque impulse also generally resembles the first half of a sinusoidal pressure-wave having a fundamental frequency **fp (in hertz)** which we term the "peak excitation frequency:"

**fp = 1/[4*(rise time of base-pressure pulse in seconds)]**

The barrel's recoil-driven vibrational excitation spectrum in the frequency domain is given by the real part of the Fourier transform of this base-pressure curve in the time domain. Since we are modeling this base pressure curve as a Gaussian-shaped function of time, the transformed excitation spectrum must therefore be another Gaussian function of frequency, centered on the peak excitation frequency **fp** and having a spread function **Sigma(hertz)** inversely related to **Sigma(µ-sec)** of its equivalent time-domain Gaussian driving function:

**(2π)*Sigma(hertz) = 1,000,000/[Sigma(µ-sec)]**

or    **Sigma(hertz) = 159,154.94/[Sigma(µ-sec)]**.

If we model the rifle barrel mechanically as a "long, slender rod" of an isotropic steel material, we can use engineering handbook formulations to calculate its response to this forced shear-wave initial distortion. Specifically, the rifle barrel is modelled as a thick-walled, linearly tapered, hollow cylindrical cantilever beam having a clamped end at its receiver junction and a free end at its muzzle. The model of the rifle barrel being used here includes a reduced diameter barrel tenon, a possible cylindrical chamber swell portion, a possible constant-rate

(linear) taper toward the muzzle, and possibly with both fixed-position and adjustable-position muzzle masses attached. These two types of muzzle attachments are each modeled as point masses with their CG locations $X_{CG}$ specified relative to the muzzle. The empty bore and chamber volumes are each considered to be cylindrical here and are removed in calculating the volume of the barrel. The barrel tenon itself is not used in vibrational calculations because it is behind the front face of the receiver.

A properly inialized interior ballistics program such as QuickLOAD© gives us the time of bullet engravement, the time of 60.65-percent of peak base-pressure (one sigma before the time of peak base-pressure), the time of peak base-pressure itself, and the time of bullet exit from the muzzle of our rifle barrel of specified internally rod-measured length $L_{int}$. Calculated peak base-pressure behind the bullet and the muzzle exit speed of the bullet are also available and are utilized.

We can calculate the "signaling delay" between the time the shear-wave is introduced at the receiver/barrel junction and the earliest time $t_0$ at which the muzzle of the barrel first begins to react vibrationally to this recoil-driven torque impulse:

==**Signaling Delay = Barrel Length/Shear-Wave Propagation Rate**==

Here we use the input Barrel Length $L_{ext}$ as measured externally from receiver face to muzzle. We calculate the shear-wave propagation rate along the rifle barrel as an un-tensioned "long, slender rod" from the properties of the (isotropic steel) barrel material as the square root of its shear modulus of elasticity $G$ divided by its density $\rho$. This transverse shear-wave longitudinal propagation rate is about **3054 meters per second** (or **10,020 feet/second**) for 416R stainless steel rifle barrels.

The muzzle begins to vibrate sinusoidally in a longitudinal vertical plane as soon as the leading edge of the upward bending torque (shear-wave) signal reaches it at the muzzle vibration start time $t_0$. These sinusoidal transverse vibrations are of multiple standing-wave modes $n$, all starting simultaneously, with each vibration mode continuing at its own specific mode frequency $f_n$ which we calculate from handbook data for the barrel as a tapered cantilever beam including possible muzzle-attached masses. Each of these mode frequencies $f_n$ is a naturally resonant

(constructively reinforcing) standing-wave frequency for transverse vibrations reflecting back and forth along the length $L_{ext}$ of the rifle barrel at the shear-wave speed. After **peak excitation**, these barrel vibrations damp exponentially with a ring-damping time constant characterized here as a large multiple of their round-trip time up and down the physical length $L_{ext}$ of the barrel. Here, we are using the same damping time constant for all significant vibrational mode frequencies $f_n$.

This analytical technique of abruptly switching from an initial forcing function at the moment of peak distortion to a damped oscillation function for these rifle barrel vibrations is akin to modeling the plucking of a guitar string versus the bowing of a violin string, as analogs of initial forced distortion versus continuous "pumping" of a mechanical vibration. This analytical treatment is justified here as being consistent with treating the rifle's recoil force effects as being impulsive in nature.

The actual muzzle motion is the instantaneous **algebraic sum** of the simultaneous sinusoidal vibration modes at their respective excitation amplitudes evaluated at the muzzle. The driving excitation or damping functions for the different vibration modes each vary as Gaussian or exponential functions of time which can thus be "factored out" analytically as a separation of variables.

As shown below, we combine the Gaussian driving function with an exponential vibrational decay, or damping function, as a Pulse Width Modulation function of time, by using only the increasing limb of the base-pressure function then switching to the damping function at the time of the peak base-pressure. If we used the decreasing limb of the pressure curve, the barrel vibrations would be killed out prematurely. The rifle barrel continues its oscillatory ringing long after the bullet has exited its muzzle. The only drawback with this approach is introduction of a step discontinuity in the second order (muzzle lateral acceleration) calculations at this transition time, which is itself much earlier than any reasonable bullet exit time. This transition time is when the peak base-pressure occurs, creating the peak upward bending torque on the rear of the barrel, and is thus the peak time of the transverse shear-wave being formed at the receiver face and propagating toward the muzzle.

We may seek to tune the muzzle exit times of our fired bullets to match a vibrational reversal time (or halt) in vertical muzzle motion when the muzzle is momentarily stationary relative to the fixed earth as a quasi-inertial reference system. Known side benefits of this traditional type of barrel/load tuning are minimizing vertical (transverse) kick-velocities **ΔV** imparted to our fired bullets and regularizing the muzzle pointing super-elevation angles **ϴ** for each bullet being launched. This traditional type of barrel and cartridge tuning is preferred for firing conventional jacketed lead-core match bullets in which the CG of the bullet is relatively near its point of last contact with the crown of the muzzle during the bullet's muzzle exiting process; i.e., typically less than one caliber ahead of that point of last contact. The barrels firing these bullets are often made with the slowest possible rifling twist-rates (**40 to 60 calibers per turn**) to minimize lateral throw-off with these slightly unbalanced projectiles. The ratio of the second moments of inertia $I_y/I_x$ for these bullets is relatively small (**7:1 to 10:1**), and their initial coning rates in ballistic flight are often about **65 hertz**. The integration time over which initial aerodynamic jump deflection accumulates is relatively brief (**7.7 msec**), being half the period of the first coning cycle, so their trajectory deflection angles are relatively small. Initial yaw and yaw-rate bullet attitude errors at launch are less important in subsequent ballistic flight when firing these bullets.

We can also achieve partial "compensation" for long-range gravity-drop variations due to slight variations in bullet launch velocities by tuning our expected (group mean) bullet exit times to occur a few microseconds earlier than an upward-to-downward muzzle halt, or just after a downward-to-upward muzzle reversal. This partial gravity-drop compensation is based upon an assumed (but quite likely) strong inverse correlation between variations in bullet launch velocities and variations in muzzle exit times within groups of shots. Tuned either way, muzzle motion is *slightly upward* at the nominal bullet exit time, and any somewhat faster bullets, exiting earlier than average, will be launched at slightly lower than average muzzle super-elevation angles **ϴ**. These faster-than-average bullets will require less time-of-flight to reach a given distant target and will thus suffer less gravity drop as a result, and vice versa.

Alternatively, we may seek to tune our rifle barrel and cartridge loading so as to launch a long, monolithic copper Ultra-Low-Drag (ULD) bullet with minimum initial yaw-rate, or "tip-off." We do that by tuning for bullet exit at, or near, a *zero crossing* of the **y-double-dot(t)** function where the lateral acceleration of the bullet as it clears the muzzle is minimal. The worked Excel spreadsheet example shows this type of tuning for firing our longer CNC-turned **245.3-grain** copper ULD bullets of **338 caliber** with a (QuickLOAD) calculated muzzle exit time of **1306 microseconds** from our **25.5-inch** Heavy Varmint test barrel. The best type of tuning to match any cartridge to its rifle barrel is simultaneously to achieve both the traditional minimum lateral muzzle velocity and this novel minimum lateral muzzle acceleration types of tuning. So far, this goal seems readily attainable only by using a barrel-block rifle design wherein the front of the clamped barrel-block functionally replaces the receiver face in the vibration calculations. This is an area for further exploration.

These long copper ULD bullets have $I_y/I_x$ ratios about *twice* those of conventional jacketed lead-core match bullets, and consequently they are fired from barrels having very fast twist-rate rifling (**20 to 24 calibers per turn**) for best gyroscopic and dynamic stability. The CG of our example copper ULD bullet is **1.537 calibers** ahead of its point of last contact during bullet exit. In ballistic flight, the initial coning rates of these copper bullets is typically only about **25 hertz**, or slower. Because of their much longer accumulation time intervals, aerodynamic jump trajectory deflections and significant initial yaw-drag penalties are of much greater concern in firing these CNC-turned copper ULD bullets to reach their designed performance potential.

## 2. Barrel Transverse Vibration Modes

For a uniform cantilever beam, its natural transverse shear-wave vibration mode frequencies $f_n$ are well determined, primarily by its *beam length* **L** and secondarily by its *flexural rigidity* **E\*I** and its *mass per unit length* **A\*ρ**, where **L** is the barrel's "vibrational length," **E** is Young's Modulus of Elasticity for the barrel steel, **I i**s the second moment of

cross-sectional area (**A**) anywhere along the uniform cylindrical rifle barrel, and **ρ** is the density (mass per unit volume) of the barrel steel:

$$f(n) = [1/(2\pi)]*[\lambda(n)/L]^2 *SQRT[E*I/(A*\rho)]$$

The mode natural frequency constants **λ(n)** in radians have been precisely measured empirically and are given in engineering handbooks.

For a thick-walled circularly cylindrical rifle barrel of uniform outside diameter **D** and caliber **d**, the second moment of cross-sectional area **I** is given by

$$I = (\pi/32)*(D^4 - d^4)$$

and its cylindrical cross-sectional area **A** is given at any point by

$$A = (\pi/4)*(D^2 - d^2)$$

The transverse vibration **_modes_** are numbered according to the count **n** of the vibration **_nodes_** (locations of zero vibrational amplitude) occurring over the beam length **L** for that vibrational **_mode shape_**. After the first few vibration modes, the natural mode frequencies **$f_n$** increase approximately with **$(2*n - 1)^2$** for each successively higher mode number **n**. The mode shapes **$y_n(x/L)$** for this clamped/free cantilever beam show the barrel's forced bending responses to the driving torque excitation spectrum at each particular mode frequency **$f_n$**:

$$y_n(x/L) = COSH(\lambda_n*x/L) - COS(\lambda_n*x/L)$$

$$-\sigma_n*[SINH(\lambda_n*x/L) - SIN(\lambda_n*x/L)]$$

where **COSH** and **SINH** are hyperbolic trigonometric functions, and the mode shape constants **$\sigma_n$** from the handbooks are also empirically measured. The first five mode shapes for our example rifle barrel are shown below for **x/L = 0** at the receiver face (clamped end) to **100-percent** of the vibrational length **L** just beyond the muzzle (free end):

First Five Transverse Vibration Modes
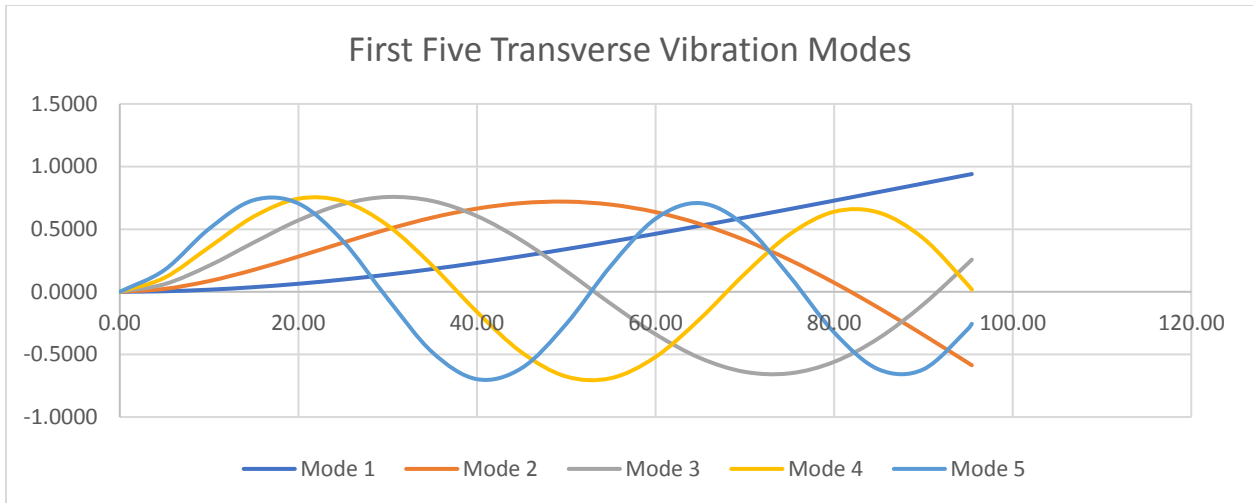
These mode shapes also show the maximum vibration amplitudes of the sinusoidal vibrations (at that mode frequency $f_n$) for each segment of the barrel (including its muzzle). By limiting excursions either above or below the neutral line, each individual mode shape shows the sinusoidal vibration envelope for each point along the beam. The clamped barrel-to-receiver joint is always a (zero amplitude) vibration node, while the free muzzle end (for a cylindrical barrel without any attached masses) is always considered to be a full-amplitude vibrational anti-node for each individual vibration mode.

Note that the actual muzzle position shown here is at about **96-percent** of the vibrational length **L** of this example for our tapered **25.5-inch** barrel having a small attached muzzle mass (a lightweight **4-ounce** muzzle brake). For a plain *tapered* barrel having no muzzle attachment, its effective vibrational length is always *shorter* than its physical length. The **Mode 1** resonant frequency *increases* with barrel taper, while the higher mode frequencies *decrease* with barrel taper.

Adding any point mass attachment at or near the muzzle always *increases* the vibrational length **L** of any barrel, including that of the tapered example shown here. The increased vibrational length **L** shown here has the effect of shifting the vibration nodes for **Mode 2** and higher-numbered modes toward the muzzle end of the actual barrel.

Each segment of rifle barrel material, including the muzzle, vibrates sinusoidally and simultaneously in a vertical plane at all significant mode frequencies $f_n$. At the muzzle, each mode frequency vibration initiates at

the first instance of the forcing shear-wave reaching the muzzle (at $t_0$). Thereafter, these independent vibratory motions mechanically combine at each particular location along the barrel (including at the muzzle) as the *algebraic sum* of the various mode-frequency motions. Note that, at the muzzle, each odd-numbered mode vibration starts out going positive (upward), while the even-numbered modes each starts out going negative (downward) at $t_0$ when the positive-going leading edge of the shear-wave distortion first reaches the muzzle.

In particular, the muzzle-end segment of the barrel vibrates transversely in a vertical plane according to the instantaneous *algebraic sum* of the first seven, or so, sinusoidal vibration modes (depending on the highest mode frequency $f_n$ which the driving force can effectively excite). Only the longest and limberest practical rifle barrel (e.g. a No. 1 Mk. III SMLE rifle barrel) could have any significant recoil excitation of its relatively reduced frequency **Mode 7** vibrations.

The muzzle vertical position **y(t)** is given at any time **t** after initial excitation time $t_0$ by:

$$y(t) = PW(t) * \sum_{(n=1,\,7)} \{(-1)^{n-1} * A(n) * SIN[2\pi * f(n) * (t - t_0)]\}$$

The initial muzzle excitation time $t_0$ is calculated as the sum of the input bullet engravement delay from an interior ballistics program and a calculated signaling delay based upon barrel length and material properties. All modes of muzzle vibrations initiate simultaneously at this time $t_0$. The Pulse Width Modulation function **PW(t)** and mode vibrational amplitudes **A(n)** are described later.

The actual barrel shape at the time of bullet exit is shown below for our worked example from the spreadsheet calculations:

Barrel Shape at Bullet Exit
(Micro-meters vs. percent L)
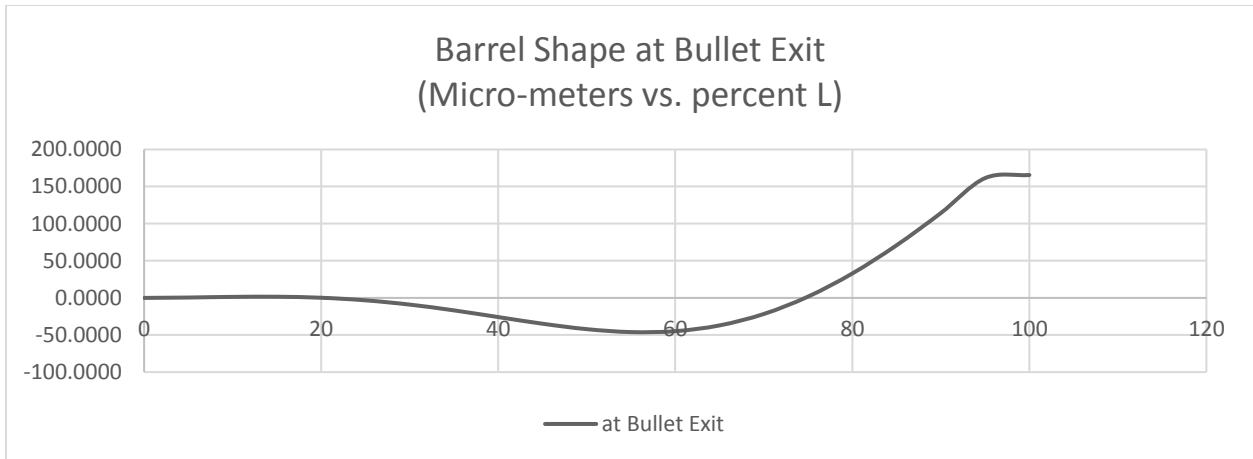
Of course, the vertical scale is greatly exaggerated here relative to the horizontal scale. The horizontal "tail" shown here to the right of the muzzle position at about **96-percent** of **L** is an artifact of Excel's curve-fitting and of my limited Excel programming skills.

The natural mode frequencies $f_n$ for a *tapered* rifle barrel including any *muzzle attachments* are given in hertz by:

$$f_n = [1/(2*\pi)]*[\lambda_n/L]^2 *SQRT[E*I_0/(M/L)]$$

where **M** is the total mass of the barrel forward of the receiver face including all attachments and **L** is the vibrationally effective barrel length.

The mode **n** frequency constants $\lambda_n$ are taken from the handbook, *Formulas for Natural Frequencies and Mode Shapes*, 1979, by Blevins for a tapered cantilever beam with clamped and free ends. These mode constants were measured experimentally. A modification to these mode frequency constants $\lambda_n$ is formulated herein for handling modestly tapered rifle barrels based on non-linear graphical data also given in Blevins.

The mode shapes are shown graphically in **Sheet 2** of the worked spreadsheet example. Note that with an upward-bending driving torque applied at the receiver end of the barrel, the muzzle end is initially moved *upward* by each odd-numbered vibration mode and *downward* by each even-numbered vibration mode.

A Gaussian Pulse Width modulation function of time, **PWG(t)**, is also calculated based on the approximately Gaussian shape of the recoil

generating base-pressure function in the time domain and the time of peak muzzle disturbance $t_{PM}$ calculated from input data.

$$PWG(t) = EXP\{-0.5*[(t - t_{PM})/sigma(time)]^2\}$$

The time of peak muzzle disturbance $t_{PM}$ is calculated by summing the input time of peak base-pressure and the calculated signaling delay.

An exponential ring-damping pulse-width function, **PWD(t)** is formulated as:

$$PWD(t) = EXP[-(t - t_{PM})/(time\ constant)] \qquad for\ t > t_{PM}$$

The decay **time constant** is formulated as a large multiple of the round-trip time for a shear-wave traversing up and down the barrel length $L_{ext}$.

A combined Pulse Width function **PW(t)** is then formed by logically combining these two time-functions:

**IF $t \leq t_{PM}$**

> **PW(t) = PWG(t)**

**IF $t > t_{PM}$**

> **PW(t) = PWD(t)**

This logical combining formulation is used to prevent the downward limb of the recoil driving function **PWG(t)** from prematurely damping out the vibrational ringing of the barrel which continues long after bullet exit.

Muzzle vertical position in microns (**micro-meters**), **y(t)** is then calculated and plotted for each microsecond of reasonably possible rifle bullet exit times, out to **t = $t_0$ + 2.000 milliseconds**. This table of calculated muzzle positions is then *differenced* to form a table of muzzle velocities **y-dot(t)** given in meters per second (**m/sec**) centered on each microsecond of possible bullet exit times. Then, this velocity table is itself *differenced* to form a table of muzzle accelerations **y-double-dot(t)** given in meters per second squared (**m/sec$^2$**) for each microsecond of possible exit times. Graphs of these tables are shown in the next section below for this example case.

The excitation spectrum calculations are shown for a worked example in **Sheet 3** of the available Excel workbook. The mode vibration Peak

Amplitudes $A_n$ at the muzzle are found by multiplying a calculated **Mode 1** excitation amplitude by the relative amplitudes from the excitation spectrum for each mode frequency $f_n$ and by a **Phase Adjustment** factor accounting for the actual muzzle location sometimes being less than the vibrational length **L** from the receiver face. The sinusoidal mode-shape vibration equations (as given in Blevins) for all modes (including **Mode 1**) are normalized for unit response at the muzzle end.

The muzzle excitation amplitude is calculated for **Mode 1** from basic physics:

$\quad$ **y(t) = Mode 1 muzzle position at time t**

$\quad$ $\mathbf{y(max) = 0.5*(d^2y/dt^2)*[\Delta t]^2}$ $\qquad$ **[Constant acceleration]**

$\quad$ $\mathbf{\Gamma_{Max} = d_{CG}*P_b*[(\pi/4)*d^2]}$ $\qquad$ **[Peak driving torque]**

$\quad$ $\mathbf{\Gamma_{Max} = I_y(rcvr\ end)*(d\omega/dt)}$ $\qquad$ **[ω is angular velocity]**

$\quad$ $\mathbf{I_y(rcvr\ end) = (1/3)*M*L^2}$ $\qquad$ **[Cylindrical barrel]**

$\quad$ $\mathbf{\Delta t = \sigma(t)*SQRT[2\pi] = 2.50663*\sigma(t)}$

$\quad$ $\mathbf{d\omega/dt = (1/L_{ext})*d^2y/dt^2 = 2*y(max)/\{L_{ext}*[2.50663*\sigma(t)]^2\}}$

$\quad$ $\mathbf{d\omega/dt = 3*\Gamma_{Max}/(M*L^2)}$

$\quad$ <mark>$\mathbf{y(max) = (3\pi)*[\sigma(t)]^2 *[\Gamma_{Max}*L_{ext}/(M*L^2)]}$</mark>

Note that **2.50663*σ(t)** is the time duration **Δt** of a square-wave impulse function with enclosed area equal to the area under the Gaussian curve:
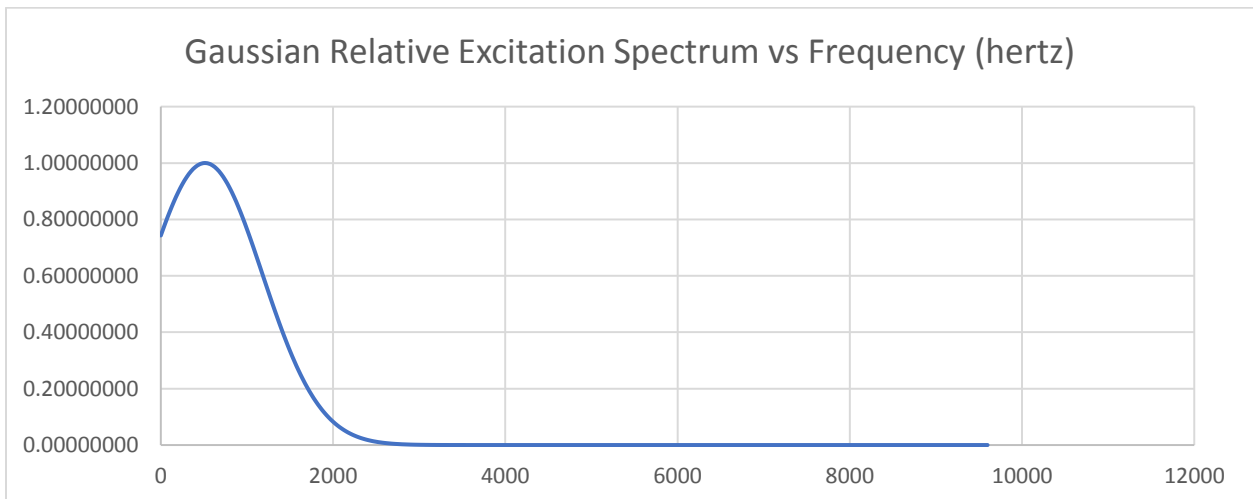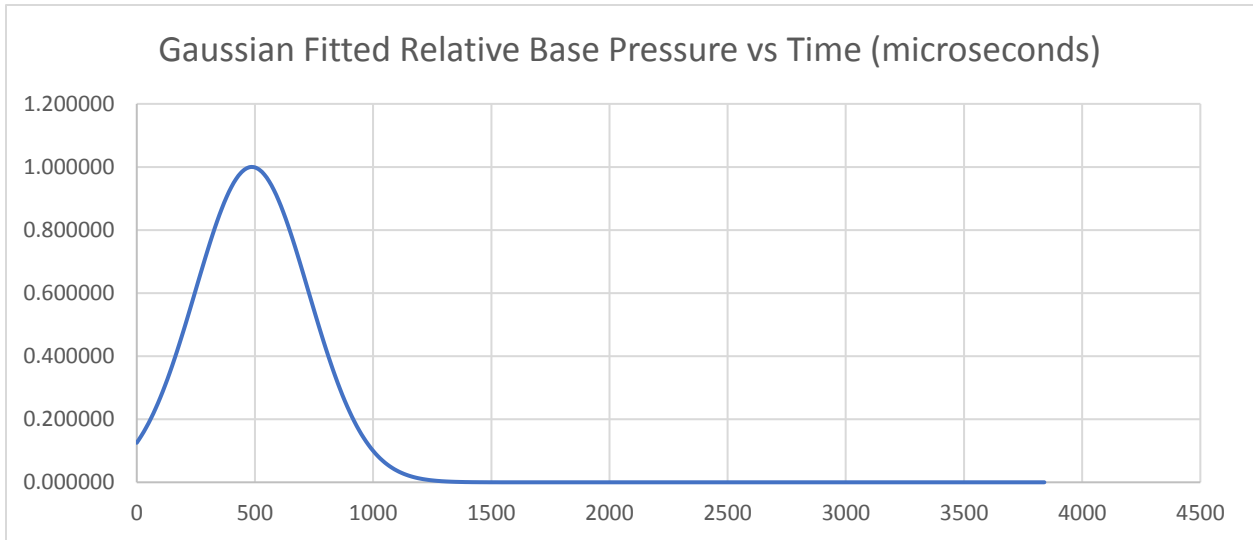
$$\mathbf{\Gamma_{Max}*\Delta t = \int_t \Gamma(t)*dt = \Gamma_{Max}*[\sigma(t)*SQRT(2\pi)] = \Gamma_{Max}*2.50663*\sigma(t)}$$

We are treating the total torque impulse $\mathbf{\int_t \Gamma(t)*dt}$ as being equivalent to applying the peak torque $\mathbf{\Gamma_{Max}}$ constantly for just **2.50663*σ(t)** seconds.

This maximum muzzle displacement **y(max)** calculated for **Mode 1** is then also used as the maximum possible muzzle displacement for each individual higher numbered vibrational mode **n**.

The peak Relative Excitation Amplitudes **REA(n)** are found for each mode frequency $f_n$ from the Gaussian excitation spectrum in the frequency domain:

$$\text{REA(n)} = \text{EXP}\{-0.5*[(f_n - f(peak))/sigma(hz)]^2\}$$

Gaussian Fitted Relative Base Pressure vs Time (microseconds)

Gaussian Relative Excitation Spectrum vs Frequency (hertz)

## 3. Barrel Taper and Muzzle Attachments

The handbook calculations of muzzle position as a function of ongoing time **y(t)** are quite accurate for cylindrical rifle barrels having uniform outside diameter **D** and having no muzzle attachment(s). We have formulated extensions of these calculations to handle those target rifles typically having moderately straight-tapered barrels, as a *Heavy Varmint* profile barrel for example, and having fixed-position (muzzle

brake) and/or adjustable-position (tuner) muzzle attachments. These extended formulations collapse exactly to the handbook natural vibration mode formulations for a uniform cantilever beam with no attached muzzle masses whenever the user-specified barrel dimension and attachment mass values describe such a barrel.

The vibrationally equivalent system has mass $M_1$ equal to the total mass of the actual rifle barrel $M_0$ plus its muzzle attachment $m$. The vibrational length $L_1$ of the vibrationally equivalent tapered cantilever beam is found by summing the second moments of inertia $I_{END}$ of the barrel and its attachment $m$ about the receiver end of the barrel and solving for the equivalent length $L_1$ of the assembly. Except in calculating the volume of the steel barrel and thence its mass $M$, the exact caliber of the bore through the rifle barrel has little effect (<0.03 percent) on the transverse shear-wave vibrations of a typically heavy target rifle barrel. So, the effect of the barrel being somewhat hollowed out is ignored. [The fiber of material connecting cross-sectional centroids of a beam is neither stretched nor compressed under bending load, so it contributes nothing toward the overall rigidity of that beam.]

If we consider all second moments of inertia I to be taken about the same transverse horizontal axis through the receiver/barrel junction, we can sum the moments of inertia for the component pieces of the plain barrel and the attached muzzle brake to find that of the combination. Furthermore, we can divide the moment of inertia of the plain tapered barrel into its tapered barrel part $I_{taper}$ (before and after adding the muzzle brake attachment $m$) and its possible cylindrical chamber swell part $I_{cs}$. So, the total moment of inertia for the combination can be written as

$$I_{1taper} + I_{cs} = I_{0taper} + I_{cs} + m_{mb}*(L_{ext} + X_{CG})^2$$

Since we are not changing the barrel's chamber swell in adjusting externally measured length $L_{ext}$ to its equivalent vibrational length $L_1$ with the addition of the muzzle brake $m_{mb}$, the moment of inertia of that chamber swell portion $I_{cs}$ remains fixed, and we are only "stretching" the tapered part of any tapered barrel to account for adding the muzzle attachment. Thus,

$$I_{1taper} = I_{0taper} + m_{mb}*(L_{ext} + X_{CG})^2$$

To find the second moment of inertia $I_{taper}$ about the receiver end of the heavy, uniformly tapered portion of the rifle barrel itself, we make use of the handbook formulation for the transverse radius of gyration **k** about a transverse axis through the large end of the frustum of a cone:

$$I_{0taper} = M_0*k_0^2$$

where     $M_0$ **=** Mass of the barrel

$$k_0^2 = 0.1*L_{taper}^2 *[(D^2 + 3*D*d +6*d^2)/(D^2 +D*d + d^2)] + D*d/16$$

or        $k_0^2 = TC2*L_{taper}^2 + D*d/16$

and      $L_{taper} = L_{ext}$ **-** $L_{cs}$ **=** Length of the barrel taper

               **D =** Maximum (receiver-end) diameter of the tapered barrel

               **d =** Muzzle diameter of the tapered barrel **[D/2 < d < D],** and

               $TC2 = 0.1*[(D^2 + 3*D*d +6*d^2)/(D^2 +D*d + d^2)]$.

The small second term, **D*d/16**, replaces the handbook second term, **(3/80)*(D^5 – d^5)/(D^3 – d^3)**, which is not well behaved computationally as **d** approaches **D** for a cylindrical barrel example. The replacement term is the ratio of the limits of the numerator and denominator as **d** approaches **D** which correctly collapses to $D^2/16$ whenever **d** equals **D**.

Since the barrel's specified major **D** and minor **d** diameters remain unchanged while adjusting the vibrational length of a tapered barrel, the taper constant **TC2** remains the same, with or without the muzzle attachment $m_{mb}$.

Note that $I_{taper}$ is now measured about an axis through the front of the chamber swell (if any) instead of the receiver face. So, our inertia summing relationship is adjusted accordingly for this axis change:

$$I_{1taper} = I_{0taper} + m_{mb}*(L_{ext} – L_{cs} + X_{CG})^2$$

Summing the second moments of inertia about the receiver (or chamber swell) end of the barrel with a point mass $m_{mb}$ attached a short distance $X_{CG}$ from the crown of the muzzle, for the tapered portion of the barrel we have

$$M_1*k_1^2 = M_0*k_0^2 + m_{mb}*(L_{Ext} – L_{cs} + X_{CG})^2$$

with        $M_1 = M_0 + m_{mb}$.

Then, solving for the vibrationally adjusted, externally measured barrel length $L_1$ we have

$$L_1 = L_{cs} + SQRT\{(M_0/M_1)*(L_{ext} - L_{cs})^2 +$$

$$+ [(L_{ext} - L_{cs} + X_{CG})^2 - D*d/16]*m_{mb}/(M_1*TC2)]\}$$

Here, in calculating the equivalent vibrational length $L_1$ after attaching a mass $m_{mb}$ to the muzzle of the rifle barrel, we are analytically stretching the uniformly tapered portion ($L_{ext} - L_{cs}$) of the barrel without explicitly changing its mass $M_1$ nor its end diameters $D$ and $d$. The only likely use for a barrel blank profile having a significant fraction of its length as a straight cylinder $L_{cs}$ would be a barrel intended for barrel-block mounting into the stock. In that case, the front of the barrel-block should take the place of the receiver face here. The receiver should be free-floating in the stock, and the scope should be cantilever mounted to the barrel-block. The barrel-block transfers the recoil force to the rifle stock.

This calculation is repeated for adding the second muzzle attachment $m_{tuner}$, except for starting with the previous resulting subtotal mass $M_1$ and vibrational length $L_1$.

Attaching any mass $m$ at or near the muzzle of a rifle barrel will always lower the natural mode frequencies $f_n$ as if that barrel were of longer vibrational length $L_1$. The ratio of the actual barrel length $L_{ext}$ to its greater vibrational length $L_1$ shows how attaching a barrel mass always shifts the vibrational node points toward the muzzle end of the rifle barrel.

As shown in **Sheet 1** of the available Excel workbook, we accept input of barrel dimensions similar to those used to describe match-grade barrel blanks and calculate the volumes of each portion of the barrel, tenon, chamber swell, taper, and the empty bore and chamber.
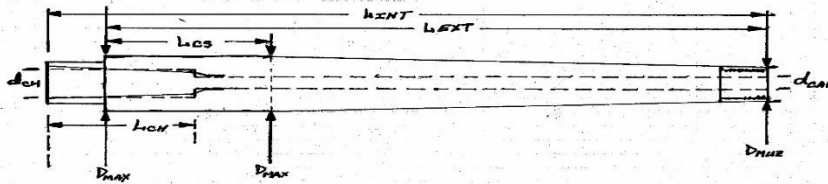
The mass of the barrel **M$_{bar}$** ahead of the receiver face is then calculated from its total steel volume and the input density **ρ** for that type of barrel steel. We use the externally measured barrel length **L$_{ext}$** for vibration calculations. [The internal rod-measured barrel length **L$_{int}$** is needed for QuickLOAD] So, before considering any possible muzzle attachments, we start with:

$$M = M_{bar}$$

$$L = L_{ext}$$

Muzzle attachments are modeled as point masses (**M$_{sub}$**) with their CG axial locations (**X$_{sub}$**) given relative to the muzzle as specified inputs. Fixed-position attachments are labeled (subscripted) **mb** for "muzzle brake," and adjustable-position attachments are labeled **tuner** for "barrel tuner," although either could be any other type of muzzle attachment. The rotational inertia of any mass attached to the muzzle end of the barrel is ignored, at least for now. [A "point-mass" has **zero** second moments of inertia about each of its principal axes.]

Blevins also gives a "one percent accurate" formulation for the **Mode 1** vibration frequency **f$_1$** for an attached point mass with its CG located exactly at the free end of a uniform cantilever beam. This formulation for **f$_1$** was evaluated numerically as a cross-check on the more flexible and analytically useful formulation described above. The cross-check **Mode 1** frequency calculation was **46.131 hertz**, versus **45.555 hertz** calculated our way for a cylindrical rifle barrel with a point mass attached with its CG exactly at the muzzle and weighing **25 percent** of the barrel weight. This **f$_1$** difference, **1.266 percent**, is less for lighter barrel

attachments, but does not go quite to **zero** for a zero-mass attachment at the muzzle. This cross-check is considered to be satisfied, given its stated accuracy limits.

Following Blevins, the controlling outside diameter **D** for the tapered cantilever beam is the (maximum) OD of the barrel abutting the receiver face $D_{max}$, and the controlling cross-sectional area **A** is calculated there as well. However, since the area **A** is no longer invariant over the length of the tapered barrel, instead of formulating the "mass per unit length" needed in calculating the mode frequencies as $A*\rho$, we simply divide the total mass **M** of the barrel assembly by its calculated vibrationally effective barrel length **L**. We must also adjust the formulation for the areal second moment **I** to be calculated at the junction with the receiver face as $I_0$:

$$I_0 = (\pi/32)*(D_{max}^4 - d_{ch}^4)$$

where $d_{ch}$ is the inside diameter of the chamber at the axial location of the receiver face as measured at that location on a fired cartridge case. The input value of $d_{ch}$ must be greater than, or equal to, the bore ID (or caliber) **d**, but well less than $D_{max}$, of course. [Continue to use the caliber **d** instead of $d_{ch}$ here with barrel-block rifles.]

Blevins graphically gives non-linear values for the first three mode frequency constants $\lambda_n$ as a function of the beam taper ratio $D_{max}/D_{min} = D/D_{muz}$ over values from **1** to **5** for truncated, linearly tapered cantilever beams. By restricting this linear taper range to from **1** to **2** for real rifle barrels ($D_{muz} \geq D_{max}/2$), we fit the following linear taper functions for calculating the mode frequency constants $\lambda_n$:

$$\lambda_1 = 1.87510407 + (0.012267)*(D_{max}/D_{muz} - 1)$$

$$\lambda_2 = 4.69409113 + (-0.59020)*(D_{max}/D_{muz} - 1)$$

$$\lambda_3 = 7.85475744 + (-1.2162)*(D_{max}/D_{muz} - 1)$$

$$\lambda_4 = 10.99554073 + (-1.7030)*(D_{max}/D_{muz} - 1)$$

$$\lambda_5 = 14.13716839 + (-2.1889)*(D_{max}/D_{muz} - 1)$$

$$\lambda_6 = 17.27875960 + (-2.6753)*(D_{max}/D_{muz} - 1)$$

$$\lambda_7 = 20.42035225 + (-3.1617)*(D_{max}/D_{muz} - 1)$$

The taper coefficients for modes **4** through **7** are estimated based on the pattern shown graphically for the first three modes. For $D_{muz} = D_{max}$, this formulation collapses to the more accurately measured $λ_n$ values for a uniform cantilever beam. Note that while the **Mode 1** frequency *increases* with barrel taper, each higher mode frequency *decreases* with barrel taper.

It should also be noted here that similar calculations of barrel ID expansion pulses, as yet another type of barrel vibration mode, could be undertaken by those concerned with "Optimum Barrel Time" tuning. Those bore expansion pulses are also shear-wave vibrations propagating along the rifle barrel at the same rate as these vertical-plane transverse shear-wave vibrations and reflecting off its ends. [A shear-wave is one in which particle vibratory motion is perpendicular to the propagation direction of the wave motion.] While these bore expansion waves initiate simultaneously with the transverse waves at the time of peak base-pressure, their initial peak internal barrel diameter expansions occur within the barrel at the bullet base location (a few inches in front of the receiver face) at the instant of peak base-pressure behind the bullet instead of at the receiver face as with the recoil-induced torque. So they must always remain several microseconds out of phase with these transverse shear-wave vibrations even after many reflections back and forth. [Bullet contact pressure increases the internal barrel expansion usually calculated using Lamé's Equation considering only the base-pressure driving the bullet. This increase is a factor **(1 + $μ_{bullet}$)** where $μ_{bullet}$ **< 0.5** is Poisson's Ratio for the bullet core material.]


## 4. Gravity Droop of Barrel

We do not need to formulate here the significant gravity droop of the rifle barrel with its muzzle attachments because that drooping does not significantly affect the muzzle motions of a typical target rifle barrel during recoil. In flat firing, the presence or absence of the earth's gravitational field does not affect the recoil-forced barrel distortions nor its subsequent ringing muzzle vibrations. All transverse barrel distortions and vibrations work equally well with a gradually curved barrel in the earth's gravity field as they would with the same rifle barrel fired

perfectly straight in the zero-g of earth orbit. In flat firing on earth, the static neutral point of muzzle position is simply displaced downward by a few thousandths of an inch affecting point of aim and point of impact consistently for each shot. A similar argument can be made for neglecting the downward bias in muzzle pointing angle at bullet exit due to gravity droop. These effects are well accommodated during the "zeroing" of the rifle's sighting system in ambient firing conditions.

We are similarly ignoring the dynamic internal pressure "stiffening" of the rifle barrel during firing, which works dynamically to reduce its gravitational droop at bullet exit, because of the relatively thick walls of our target rifle barrels—as opposed to those of typical artillery tubes, for example. The "Bourdon tube" hoop-stress effect, which slightly increases **Mode 1** upward displacement at the time of bullet exit, is negligibly small here for our circularly concentric, very thick-walled, steel target rifle barrels.

## 5. Worked Example

A "live" Excel workbook of four spreadsheets which perform these calculations is freely available as an email attachment upon request from the author. In addition to having access to a current version of Microsoft Excel, the user will also need access to a good interior ballistics program such as QuickLOAD©, which we routinely use in load development here. In particular, this analysis uses the QL definition of start time (**t = 0**) based upon the initiation of significant chamber pressure rise to the prevailing shot-start pressure. Other interior ballistics programs might use time-since-sear-break, or time-since-primer-ignition, either of which would occur earlier, and their event timings would require adjustment for use here. [Just note the time of initial chamber pressure rise attributable to powder combustion to the shot-start pressure and subtract that time from all other event times.]

The example shown is for a painstakingly assembled load in a heavy-barrel 338 Lapua Magnum test rifle using a **25.5-inch** Heavy Varmint profile Schneider P5 barrel of 416R stainless steel made with an experimental **7.0-inch** twist rate (**20.7 calibers per turn**). The muzzle end of the barrel is threaded **0.75-inch by 24 TPI** for accepting muzzle attachments such as the lightweight (**4.127 ounce**) Barrett MRAD

muzzle brake used here. The bullet is a developmental CNC-turned, **245.3-grain** monolithic copper Ultra-Low-Drag (ULD) projectile propelled by 92.0-grains of the VihtaVouri N565 temperature-stabilized powder incorporating an anti-copper-fouling additive. The copper bullets are base-drilled (at **0.45 caliber**) in manufacturing to allow internal expansion for proper sealing of the powder gasses, and they consistently exit the muzzle at **2814 fps (+/- 4 fps)** as measured using an inertially triggered LabRadar unit. QuickLOAD© shows these bullets exiting the muzzle at **t = 1314 microseconds**. All firing tests are conducted in a high-volume indoor test range on targets at 105 yards from a massively sturdy firing bench. [The current spreadsheet shows tuning for a shortened and re-chambered version of this Schneider barrel. The powder load is adjusted to 96.0 grains, reflecting the reduced shot-start pressure required with the new 1.5-degree throat angle.]
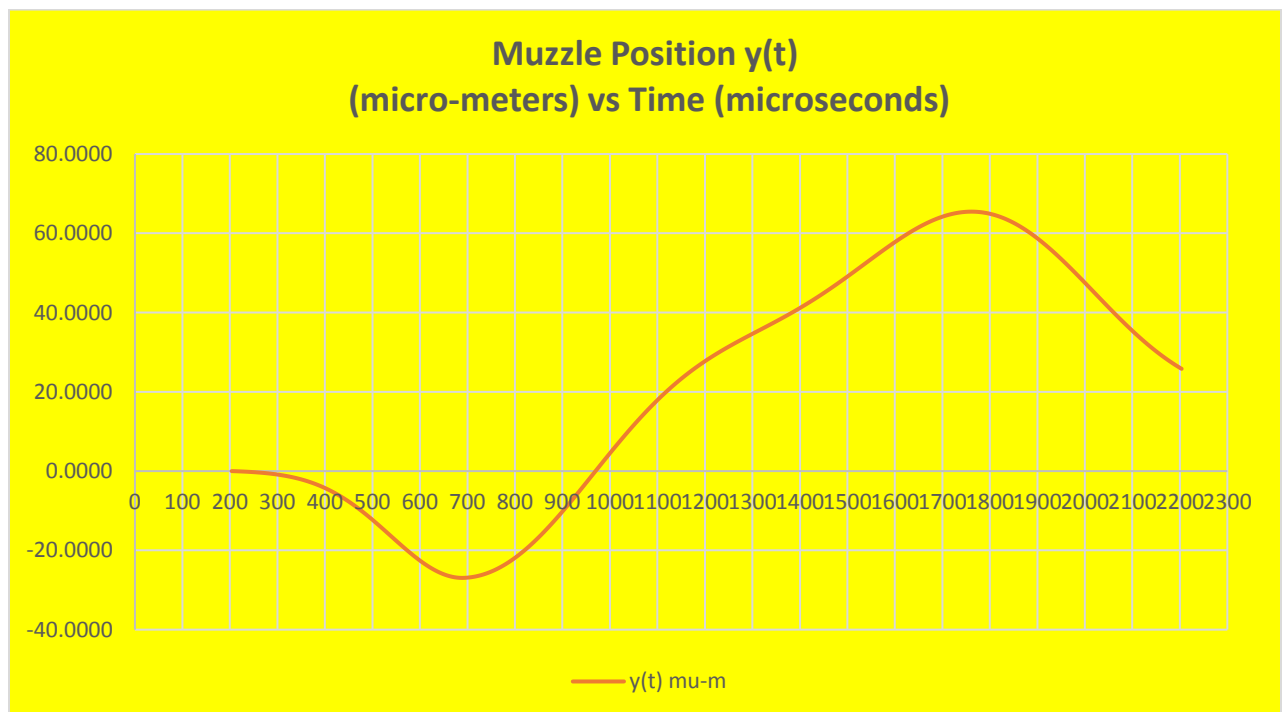
**Sheet 1** of the available Excel workbook is for the ***Data Inputs***, **Sheet 2** shows the calculation of the ***Mode Frequencies and Shapes***, **Sheet 3** shows the relative ***Excitation Spectrum***, and **Sheet 4** shows the ***Calculated Results***, both numerically and graphically, including graphs of muzzle vertical position **y(t)** in micro-meters versus time **t** in microseconds, muzzle velocity **y-dot(t)** in meters/second, and Muzzle lateral acceleration **y-double-dot(t)** in meters/second squared. The table of ***Event Times*** shows the QL-calculated bullet exit occurring at **t = 1306 microseconds** when the lateral acceleration **y-double-dot(t)**, and thus the lateral force [**F = m*a**, with **m** being the mass of the projectile] on the bullet leaving the muzzle, is essentially **zero** (**< +/- 2.5 m/s²**). The rather large lateral acceleration values shown at other times are primarily attributable to the great stiffness (**E*I**) of the rigid large-diameter steel barrel.
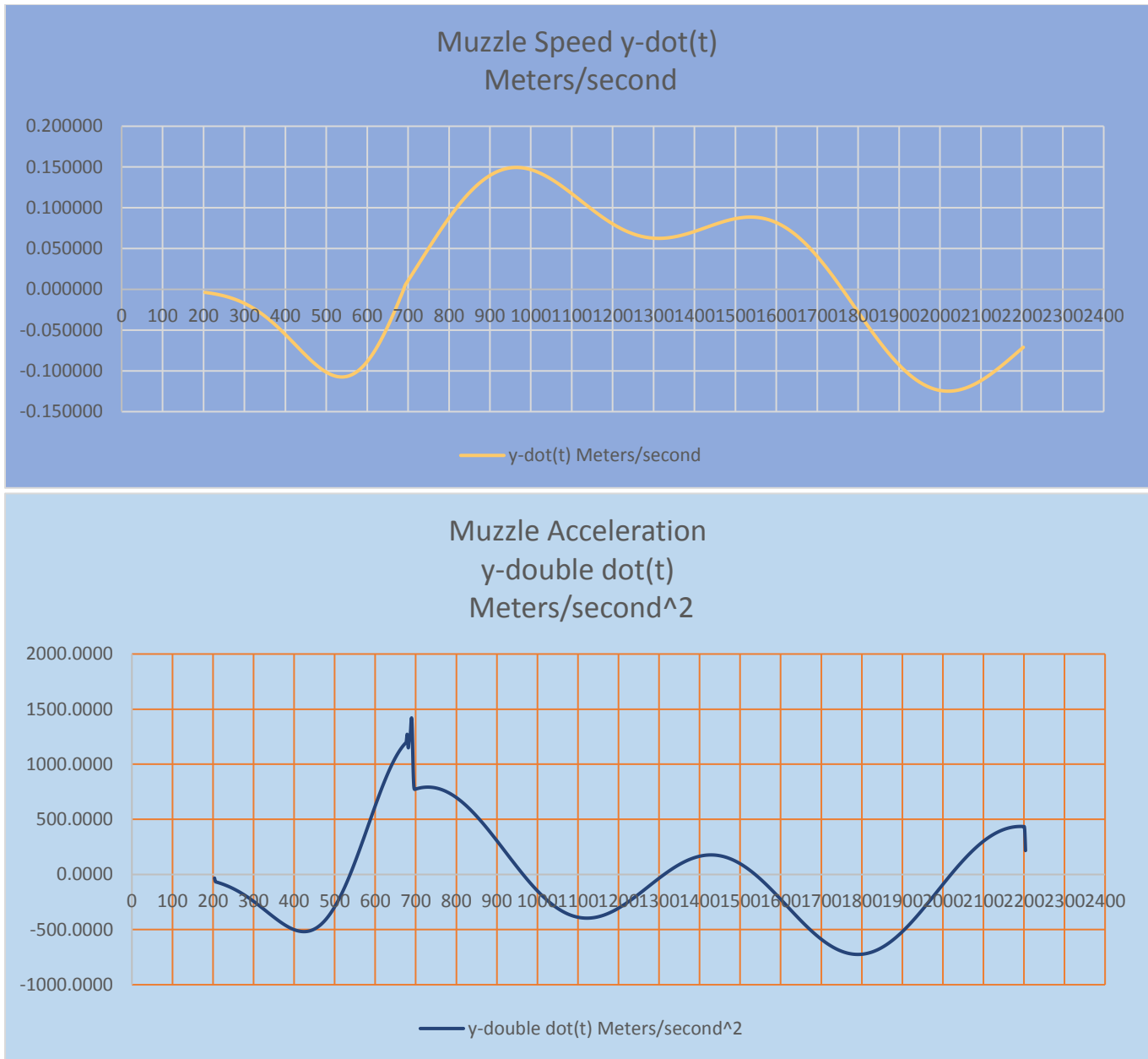
The large lateral force exerted upon the bullet of mass **m** during its muzzle exit process, which tends to occur with traditional barrel tuning for bullet exit at a muzzle vibrational reversal time, causes significant "tip-off" yaw-rates when firing long copper ULD bullets. This longer type of bullet typically has its CG located more than one caliber ahead of its point of last contact while exiting the bore. The resulting initial yaw-rate of tumbling is then subject to amplification by the reverse aerodynamics encountered by the bullet in transiting the muzzle-blast zone before

commencing ballistic flight. This significant initial ballistic yaw-rate then causes poor accuracy and excess air drag in subsequent ballistic flight-- attributable primarily to the slower coning rates of these longer bullets fired from faster twist-rate barrels.

However, one should not peremptorily dismiss any of these tiny-appearing vibrational amplitudes, muzzle speeds, and lateral accelerations as being so small that they can safely be ignored. They are perfectly capable of wrecking the expected performance of good rifles, bullets, and ammunition. Untuned combinations exhibit less than stellar target accuracy and smaller than necessary measured Ballistic Coefficient (BC) values having far greater shot-to-shot variability than otherwise necessary.

The attached plots show barrel-to-load tuning for bullet exit at essentially **zero** lateral acceleration at **1306 microseconds**, bullet exit time. This is for an experimental test firing to launch long, monolithic copper ULD bullets with minimum initial yaw-rate.



Muzzle Position y(t) (micro-meters) vs Time (microseconds)

## Muzzle Speed y-dot(t)
## Meters/second

y-dot(t) Meters/second

## Muzzle Acceleration
## y-double dot(t)
## Meters/second^2

y-double dot(t) Meters/second^2

The step-discontinuity in muzzle lateral acceleration is a formulation artifact caused by suddenly switching from recoil-forced distortion of the barrel to damped ringing at the instant of peak muzzle disturbance at **t = 700 microseconds** here. No actual rifle bullet could exit the muzzle of a **25.5-inch** barrel anything like this quickly. Note that the peak upward acceleration of the muzzle is an impressive **125 "G's"** of **9.80665 m/sec²** each in this example.

A photograph of one of the completed muzzle brake and tuning assemblies tested is shown below.



## 6. Summary

If you find that you lack sufficient control authority in tuning your bullet weight and propellant load choices for bullet exit at or very near one of your barrel's plotted muzzle reversal times or zero-force crossing times, your choice of rifle barrel profile, length, and weight/position of muzzle attachment simply cannot optimally fire bullets of your selected length, caliber, chambering, and bullet-weight range. Shortening an existing slightly too long barrel can often allow the desired load tuning with the desired bullet, powder, and muzzle attachment. Adding an additional muzzle-attached barrel mass can vibrationally lengthen a too-short barrel for tuning. Using this analytical tool during rifle design could possibly avoid making costly mistakes in rifle building.

Using the spreadsheet calculations, one can identify particular combinations of barrel dimensions, rifle building techniques, and muzzle attachments which will result in the muzzle exit time for a particular cartridge and bullet being simultaneously at near zero lateral acceleration and near zero lateral velocity of the muzzle. This type of "super-tuning" would be advantageous in firing any type of rifle bullet.